Journal of Thermal Engineering
Yildiz Technical University Press, Istanbul, Turkey
Vol. 1, Special Issue 1, pp. 251-262, February, 2015.

http://eds.yildiz.edu.tr/journal-of-thermal-engineering/Articles
Manuscript Received November 12, 2014; Accepted November 19, 2014

This paper was recommended for publication in revised form by Editor in Chief Ahmet Selim Dalkilic

DETERMINATION OF FIN PITCHES FOR MAXIMUM PERFORMANCE INDEX OF L-FOOTED SPIRAL FIN-AND-TUBE HEAT EXCHANGERS

Parinya Pongsoi
Fluid Mechanics, Thermal Engineering and Multiphase Flow Research Lab. (FUTURE), Department of Mechanical Engineering, Faculty of Engineering, King Mongkut's University of Technology Thonburi, Bangmod, Bangkok 10140, Thailand.

***Somchai Wongwises**
Fluid Mechanics, Thermal Engineering and Multiphase Flow Research Lab. (FUTURE), Department of Mechanical Engineering, Faculty of Engineering, King Mongkut's University of Technology Thonburi, Bangmod, Bangkok 10140, Thailand.

Keywords: fin, tube, heat transfer, heat exchanger, optimum, air-water
** Corresponding author: Phone: +6624709115,*
E-mail address: somchai.won@kmutt.ac.th

ABSTRACT

In this study, the fin pitches of L-footed spiral finned tube heat exchangers were determined for maximimum performance index. The experiments were done at various fin pitches (f_p = 2.4, 3.2, and 4.2 mm) under the range of high Reynolds numbers (5,000–15,000). The test sections had a parallel and counter cross-flow arrangement having the number of tube row of 2. The two working fluids were the ambient air and hot water. The performance indexes (ζ_1, ζ_2, and ζ_3) were used to analyze the experimental data at different fin pitches. The results show that the optimal fin pitches for L-footed spiral finned tube heat exchangers are 2.4 and 3.2 mm.

INTRODUCTION

The air-side performances of conventional spiral finned tube heat exchangers have been studied by a number of researchers. The most productive studies are listed below. Genic et al. [1] investigated air-side pressure drops in conventional spiral finned tube heat exchangers with inline and staggered tube arrangements. Hamakawa et al. [2] investigated the vortex-shedding characteristics of conventional spiral finned tubes by using a smoke-wire technique. Lee et al. [3, 4] investigated the air-side heat transfer characteristics of conventional spiral finned tube heat exchangers under frosting and non-frosting conditions. They investigated these characteristics by varying the number of tube rows, the fin pitches, and the fin alignments. Empirical correlations for predicting the heat transfer performance at low Reynolds number was proposed.

The L-footed spiral fin utilizes a specialized type of fin geometry. The base of the fin has an L-shape, which can provide a large contact area and ensure a good path for heat transfer from the tube surface to the fin. It can also prevent the corrosion of the tube from the long-term operation. Despite its importance in many applications, only a few research works on L-footed spiral finned tube heat exchangers [5, 6] are existing.

An experimental investigation of the influence of fin's outside diameter (d_f) and the number of tube rows (N_{row}) at high Reynolds number was reported in Pongsoi et al. [5]. The test sections had a multipass parallel and counter cross-flow arrangement. The test was done under sensible heating conditions. Later, Pongsoi et al. [6] investigated the influence of the fin pitch (f_p) under high Reynolds numbers and found that the fin pitches had significant effects on the heat transfer and frictional pressure drop.

Previous studies on plain, annular, conventional, and crimped spiral finned tube heat exchangers found that fin pitch plays a significant role in air-side performance [7-12]. However, information on L-footed spiral fin-and-tube heat exchangers is still limited [5-6], despite their potential in waste heat recovery applications. As a consequence, this work investigates the effect of fin pitch (f_p) of L-footed spiral finned tube heat exchangers on air-side performances. A determination of f_p for the maximum performance index of L-footed spiral fin-and-tube heat exchangers will be presented. A large-diameter tube, which is very commonly used in ventilators, fan-coil units, and waste heat recovery units [13-16] is investigated.

DATA REDUCTION

An experimental apparatus and test section are shown in Figs. 1-2. The system consists of two loops: an air loop and a water loop. Ambient air and hot water were used as working fluids. The experimental system is composed of air supply loop (open wind tunnel), hot water cycling loop, test section (L-footed spiral fin-and-tube heat exchanger), instrumentation and data acquisition systems. All the tests were performed at steady state condition, temperatures of working fluid at inlet and outlet, as well as the pressure drop of the air flowing across the test section,

were measured. The geometric details of the spiral fin-and-tube heat exchangers are shown in Table 1.

The air-side heat transfer rate is given by:

$$Q_a = m_a c_{P,a} \Delta T_a \quad (1)$$

which $\Delta T_a = T_{a,in} - T_{a,out}$.

The water-side heat transfer rate is given as:

$$Q_w = m_w c_{P,w} \Delta T_w , \quad (2)$$

which $\Delta T_w = T_{w,in} - T_{w,out}$.

Eq.3 is used for data reduction.

$$Q_{ave} = \frac{Q_a - Q_w}{2} . \quad (3)$$

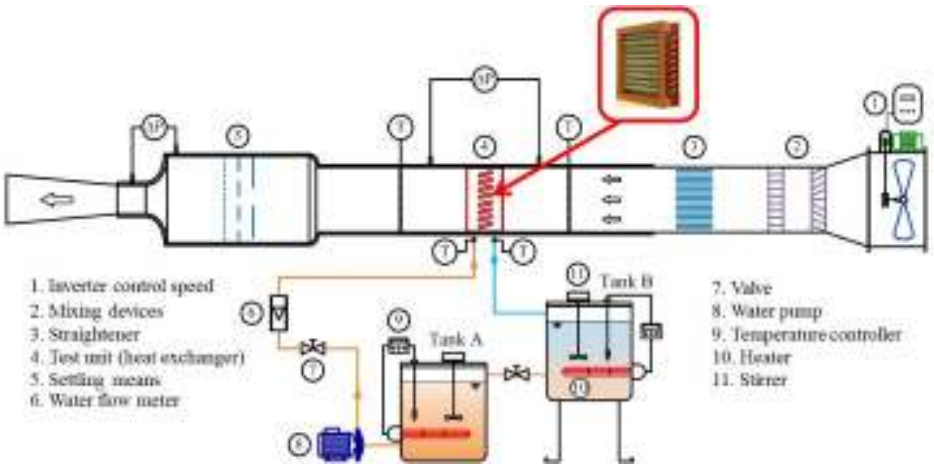

FIGURE 1 SCHEMATIC DIAGRAM OF THE EXPERIMENTAL APPARATUS

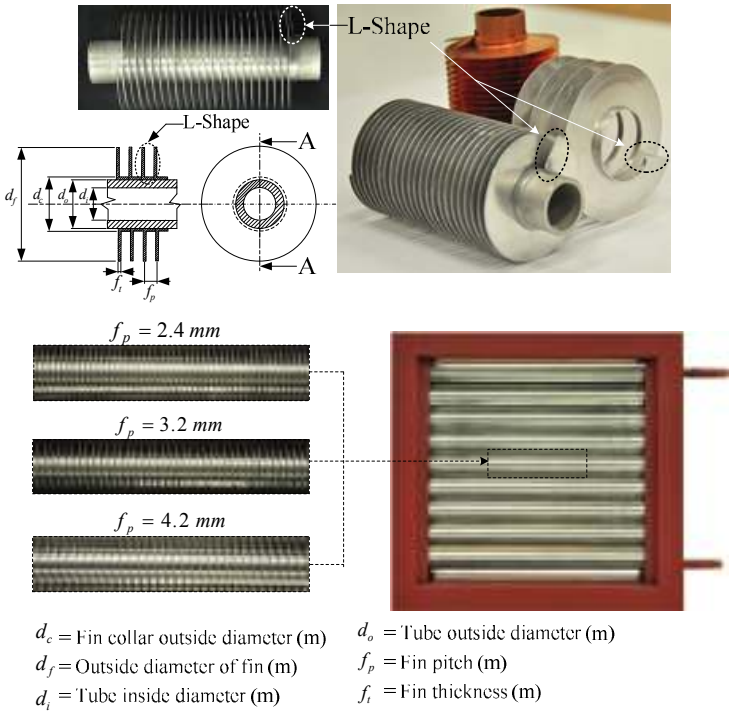

FIGURE 2 PHOTOS OF THE TESTED L-FOOTED SPIRAL FIN AND TUBE HEAT EXCHANGERS AND SCHEMATIC DIAGRAM OF THE L-FOOTED SPIRAL FIN.

TABLE 1 DETAILED GEOMETRIC PARAMETERS OF THE TEST SECTIONS

No.	Fin type	$d_i\,(mm)$	$d_o\,(mm)$	$d_c\,(mm)$	$d_f\,(mm)$	$f_t\,(mm)$	$P_L\,(mm)$	$P_T\,(mm)$	n_t	N_{row}	$f_p\,(mm)$
1	L-footed	13.5	16.35	16.85	34.8	0.25	35	39	9	2	**2.4**
2	L-footed	13.5	16.35	16.85	34.8	0.25	35	39	9	2	**3.2**
3	L-footed	13.5	16.35	16.85	34.8	0.25	35	39	9	2	**4.2**

Notes: Staggered layout are used.

Remarks: d_c = Fin collar outside diameter, d_f = Outside diameter of fin, d_i = Tube inside diameter, d_o = Fin outside diameter, f_p = Fin pitch, f_t = Fin thickness, n_t = Number of tubes, N_{row} = Number of tube rows, P_L = Longitudinal tube pitch, P_T = Transverse tube pitch.

The total thermal resistance (or *1/UA*) is the summation of each of resistances (conduction and convection resistances), as follow:

$$\frac{1}{UA}=\frac{1}{h_iA_i}+\frac{ln(d_o/d_i)}{2\pi k_tL}+\frac{ln(d_c/d_o)}{2\pi k_fL}+\frac{1}{\eta_oh_oA_o}. \quad (4)$$

Multipass parallel cross-flow
For (N_{row} = 2):

$$\varepsilon_p=\left(1-\frac{K}{2}\right)\left(1-e^{-2K/C_A^*}\right), K=1-e^{-NTU_A(C_A^*/2)} \quad (5)$$

Multipass counter cross-flow
For (N_{row} = 2):

$$\varepsilon_c=1-\left[\frac{K}{2}+\left(1-\frac{K}{2}\right)e^{2K/C_A^*}\right]^{-1}, K=1-e^{-NTU_A(C_A^*/2)} \quad (6)$$

The details of the water-flow circuit, and a geometric of the L-footed spiral finned tube heat exchanger are illustrated in Fig. 3.

For (N_{row} = 2):

$$\varepsilon_{pc}=\frac{\varepsilon_p+\varepsilon_c}{2} \quad (7)$$

where $C^*=C_{min}/C_{max}$ is equal to C_c/C_h or C_h/C_c, depending on the values of the hot and cold fluid heat capacity rates.

$$C_{min}=\begin{cases}C_h;C_h<C_c\\ or\\ C_c;C_c<C_h\end{cases} \quad (8)$$

as

$$Q_{max}=(mc_P)_c(T_{h1}-T_{c1}) \text{ if } C_c<C_h \quad (9)$$

or

$$Q_{max}=(mc_P)_h(T_{h1}-T_{c1}) \text{ if } C_h<C_c \quad (10)$$

$$\varepsilon=\frac{Q_{ave}}{Q_{max}} \quad (11)$$

$$NTU=\frac{UA}{C_{min}}, \quad (12)$$

so that

$$UA=C_{min}(NTU). \quad (13)$$

Gnielinski [17] proposed semi-empirical correlation of the heat transfer coefficient (h_i) in tube as follows:

$$h_i=\left(\frac{k_w}{d_i}\right)\frac{(Re_{di}-1000)Pr(f_i/2)}{1+12.7\sqrt{f_i/2}\left(Pr^{2/3}-1\right)}, \quad (14)$$

where the friction factor in tube-side is as follows:

$$f_i=(1.58lnRe_{di}-3.28)^{-2}, \quad (15)$$

where $Re_{di}=\rho V_id_i/\mu$.

The relationship of overall surface effectiveness (η_o), fin efficiency (η_f), fin surface area (A_f), and total heat transfer area (A_o) can be illustrated as follows:

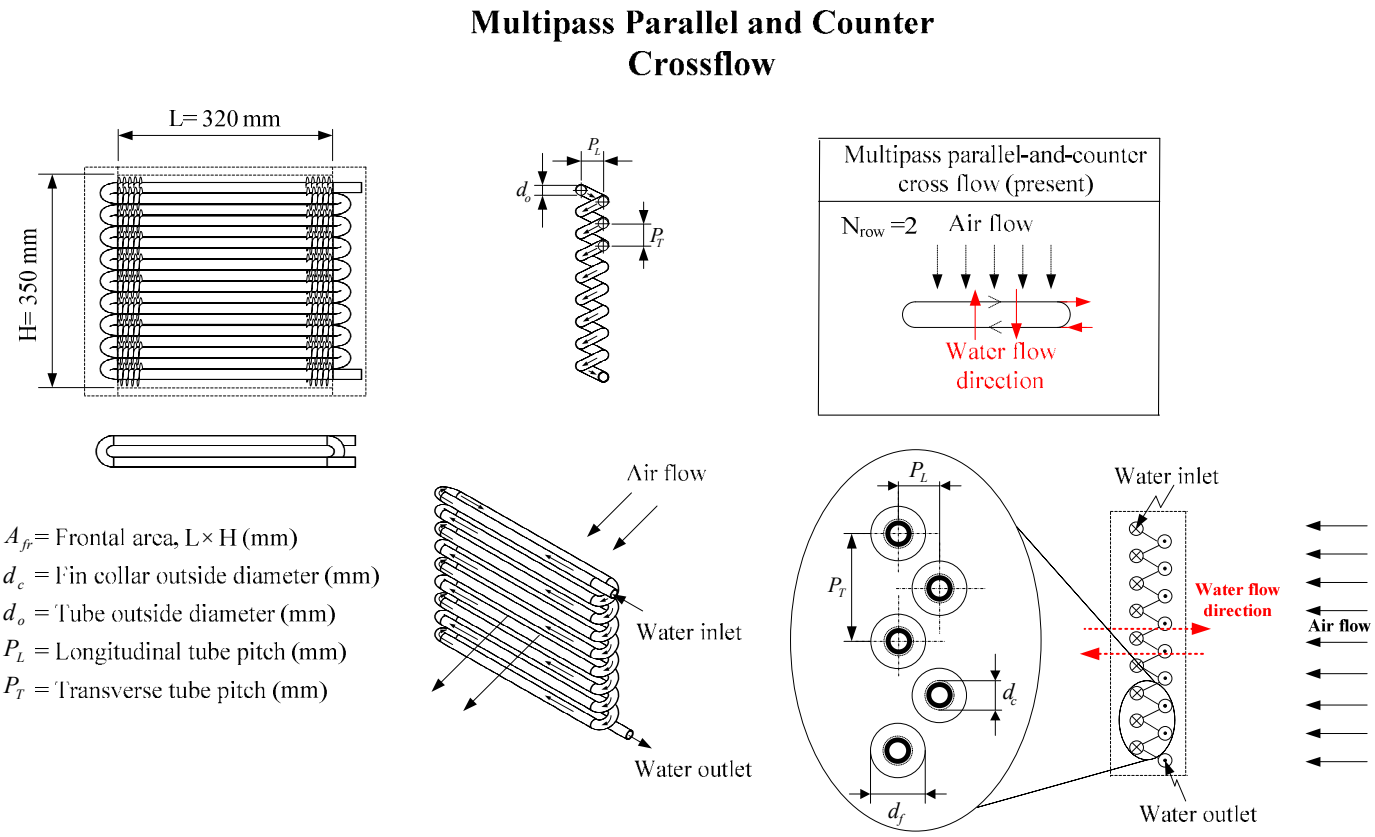

FIGURE 3 GEOMETRIC DETAILS AND SCHEMATIC DIAGRAM OF THE HEAT EXCHANGERS ALGORITHM FOR MULTIPASS PARALLEL CROSS FLOW, MULTIPASS COUNTER CROSS FLOW AND MULTIPASS PARALLEL-AND-COUNTER CROSS FLOW (× AND ● SIGNS INDICATE THAT WATER FLOWS INTO OR OUT OF THE PAPER, RESPECTIVELY).

$$\eta_o = 1 - \frac{A_f}{A_o}(1-\eta_f) \tag{16}$$

The unfinned base surface (A_b) and fin surface area (A_f) can be expressed in form of Eqs. (17) and (18), respectively:

$$A_b = n_t N_{row}\left[\pi d_o L - \left(\sqrt{f_p^2 + (\pi d_o)^2}\right)\times f_t\left(\frac{L}{f_p}\right)\right]. \tag{17}$$

The fin surface area (A_f) based on assumption of the circular fin can be determined as follows:

$$A_f = n_t N_{row}\left(\frac{L}{f_p}\right)\left[0.5\pi d_f^2 - 0.5\pi d_o^2 + \pi d_f f_t\right], \tag{18}$$

where $A_o = A_f + A_b$

Gardner [18] proposed the fin efficiency for a circular fin (Eq. (19)), it will be applied for our calculation.

$$\eta = \frac{2\psi}{\phi(1+\psi)}\frac{I_1(\phi R_o)K_1(\phi R_i) - I_1(\phi R_i)K_1(\phi R_o)}{I_0(\phi R_i)K_1(\phi R_o) + I_1(\phi R_o)K_0(\phi R_i)}, \tag{19}$$

where

$$\phi = (r_o - r_i)^{3/2}\left(\frac{2h_o}{k_f A_p}\right)^{1/2} \tag{20}$$

and where A_p is the area in the rectangular profile of the fin:

$$A_p = f_t(r_o - r_i). \tag{21}$$

The parameters R_o and R_i are given in terms of the radius ratio (ψ):

$$R_o = \frac{1}{1-\psi} \tag{22}$$

and

$$R_i = \frac{\psi}{1-\psi}\ , \tag{23}$$

where

$$\psi = \frac{r_i}{r_o}. \tag{24}$$

$$Re_{dc} = \frac{\rho_a V_{max} d_c}{\mu}\ ; \tag{25}$$

$$j = \frac{Nu}{Re_{dc} Pr^{1/3}} = \frac{h_o}{\rho_a V_{max} c_P}(Pr)^{2/3}, \tag{26}$$

where the air-side heat transfer coefficient (h_o) is obtained from Eq. (4).

The primary purpose of this study is to determine an optimized fin pitch using the performance index. The performance index is defined as the ratio of the desired output to the required input. However, three performance indices are used for analysis the optimum fin pitch: the heat exchanger performance index (ζ_1), the system performance index (ζ_2), and the dimensionless system performance index (ζ_3), each of which is described below.

The heat exchanger performance index is calculated using:

$$\zeta_1 = (Q_{ave}/\Delta P)_{\mathrm{HX}}, \tag{27}$$

where the subscript "HX" means "heat exchanger."

The system performance index is calculated using:

$$\zeta_2 = (Q_{ave}/\Delta P)_{\mathrm{Sys}}, \tag{28}$$

where the subscript "Sys" means "system."

The dimensionless system performance index is calculated using:

$$\zeta_3 = (Q_{ave}/\ W_F)_{\mathrm{Sys}}\ , \tag{29}$$

where W_F is fan power.

The actual performance of the heat exchanger relies on the cooperation between heat exchanger and fan. Hence, the heat exchanger performance index (ζ_1) quantitatively evaluates the conventional performance of heat exchangers using the ratio of the average heat transfer rate on the air side to the pressure drop across the heat exchanger. In other words, this study also investigated heat transfer performance in relationship to the influence of commercial fans on the operation of heat exchanger systems. The evaluation criteria were proposed in terms of the system performance index (ζ_2) at the operating point, which is the point of intersection between the axial fan performance curve and the system curve of the heat exchanger.

Finally, the dimensionless system performance index (ζ_3) is a modification of the system performance index obtained by dividing the average heat transfer rate by the fan power (W_F) at the operating point. In other words, the dimensionless system performance index (ζ_3) could be described as the coefficient of performance, since it represents the ratio of the desired heat transfer rate to the provided fan power $(Q_{ave}/\ W_F)_{\mathrm{Sys}}$.

The fan power is determined by the fanning friction factor (Eq. (30)), as proposed by Kays and London [19].

$$f = \left(\frac{A_{min}}{A_o}\right)\left(\frac{\rho_m}{\rho_1}\right)\left[\frac{2\Delta P \rho_1}{G_c^2} - \left(1+\sigma^2\right)\left(\frac{\rho_1}{\rho_2}-1\right)\right], \tag{30}$$

where σ is the ratio of the minimum free flow area to the frontal area, A_o is the total heat transfer area, and A_{min} is the minimum free flow area.

For Eq. (30), if the entrance and exit effects are negligible ($\rho_1 = \rho_2$ and $\rho_m = [\rho_1 + \rho_2]/2$), then the friction factor can be determined from

$$f = \frac{A_{min}\rho_m}{A_o}\left[\frac{2\Delta P}{G_c^2}\right]. \tag{31}$$

So, the fan power is

$$W_F = \frac{G_c A_{min} \Delta P}{\rho_m}. \tag{32}$$

Table 2 illustrates the accuracy of the measurements. The root mean sum square method is used to determine the uncertainties, as shown in Table 3. Moreover, this work presents the experimental results according to a primary analysis based on the energy balance. Fig. 4 shows that the energy balances between the air and water based on the ANSI/ASHRAE 33 Standards [20], indicating that $|Q_a - Q_w| \times 100 / |Q_{ave}|$ was less than 5%. All of the tested conditions are shown in Table 4.

TABLE 2 ACCURACY OF THE MEASUREMENTS

Parameters	Accuracy
Inlet-air dry-bulb temperature, ^oC	± 0.1
Pressure drop, Pa	± 0.5
Inlet-water temperature, ^oC	± 0.1
Water flow rate, LPM	± 0.4 (± 0.02 of full scale)

TABLE 3 UNCERTAINTIES OF THE DERIVED EXPERIMENTAL VALUES

Parameters	Maximum uncertainties (%)
Air-side heat transfer rate, Q_a	$\pm$5.0
Water-side heat transfer rate, Q_w	$\pm$3.4
Pressure drop, ΔP	$\pm$2.5
Frontal velocity, V_{fr}	$\pm$3.0
Reynolds number, Re_{dc}	$\pm$3.1
Colburn factor, j	$\pm$12.5
Friction factor, f	$\pm$11.1

TABLE 4 EXPERIMENTAL CONDITIONS

Inlet-air-dry bulb temperature, ^oC	31.5±0.5
Inlet-air frontal velocity, *m/s*	2-8 or Re_{dc} (5,000-15,000)
Inlet-water temperature, ^oC	55-70
Water flow rate, *LPM*	12-14

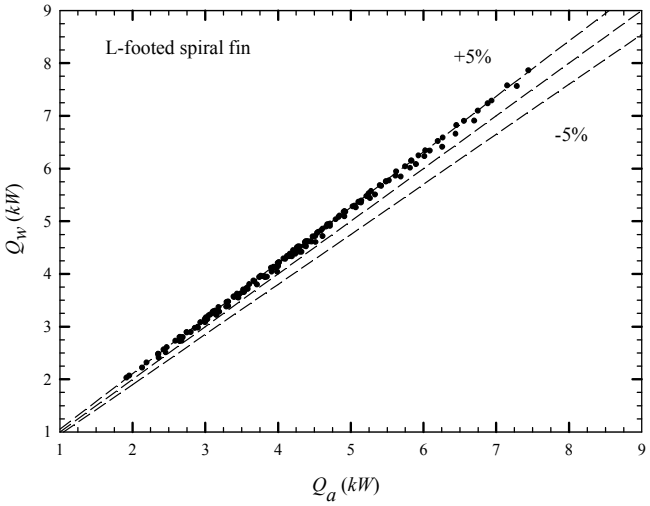

FIGURE 4 ENERGY BALANCE BETWEEN AIR AND WATER.

RESULTS AND DISCUSSION

The major finding of this study is that fin pitch had a significant effect on the maximum performance of the L-footed spiral fin-and-tube heat exchangers. The experimental results were related to the three performance indexes ζ_1, ζ_2, and ζ_3 which were the significant methodologies developed to optimize fin pitch. The average heat transfer rate (Q_{ave}) and the pressure drop across the heat exchanger (ΔP) for all of the tested samples were determined from the experimental data. The results were presented in bar charts showing the three performance indices (ζ_1, ζ_2, and ζ_3) obtained from three types of fans for three fin pitches.

The optimization of fin pitch was analyzed using these three performance indices, each of which optimized the fin pitch of the L-footed spiral fin-and-tube heat exchangers. The numerator and denominator represent the air-side heat transfer rate and pressure drop of heat exchanger, respectively. Therefore, the heat exchanger performance index (ζ_1) describes the performance of the heat exchanger. In Fig. 5(a), the effects of fin pitches on the heat exchanger performance index (ζ_1) are investigated under different inlet water temperatures and water flow rates. For a V_{fr} of 3–4 *m/s*, the results showed that fin pitch significantly influenced the heat exchanger performance index (ζ_1). As the fin pitch increased (goes from left to right) in the interval from 2.4 to 3.2 mm, the value of ζ_1 increased and the curve rose. On the other hand, as the fin pitch increased at the interval from 3.2 to 4.2 mm, the curve fell. ζ_1 became its maximum at the fin pitch of 3.2 mm. For a V_{fr} of 5–6 *m/s* and fin pitches of 2.4 and 3.2 mm, the effects of fin pitches on the value of ζ_1 are negligible. Interestingly, the heat exchanger performance index (ζ_1), which increases with decreasing air-frontal velocity, can be enhanced by up to 150% at air frontal velocities from 3 to 6 *m/s*. The trend of the heat exchanger performance index is still the same for different inlet-water temperatures and water flow-rate conditions, as shown in Figs. 5(b), 6(a), and 6(b), respectively.

In the case of the system performance index (ζ_2), we begin by analyzing only the test section, as in the analysis of ζ_1. However, ζ_2 was developed to obtain the performance index at the optimum fan operating point, with the same method as that used in previous studies [7, 12]. The system performance index presents the relationship between the heat exchanger and air supply at operating point. By themselves, then, the numerator (Q_{ave}) and denominator (ΔP) are considered to be based on the relationship between the system curve of the L-footed spiral fin-and-tube heat exchangers with different fin pitches (2.4 to 4.2 mm) and the axial commercial fan curve (P-Q fan curve A to C). The ratio of the average heat transfer rate to the pressure drop at this operating point is represented as ζ_2. The operating point represents a specific point within the operational characteristics of a device. The fin pitch has significant effect on the system performance index (ζ_2), as related to the actual fan curve, as illustrated in Fig. 7.

The major findings revealed no significant difference in the ζ_2 between a fin pitch of 2.4 and 3.2 mm. However, the system performance indices (ζ_2) for f_p = 2.4 and 3.2 mm are significantly higher than that for f_p = 4.2 mm by about 20% for every fan curve. The purpose of the fin pitches at 2.4 and 3.2 mm is to increase the system performance index (ζ_2) and improve the optimum fin pitch for L-footed fins. The results also demonstrated that the system performance index (ζ_2) increases as the power input decreases to the fan. This section suggests the need for a more careful analysis of the fan curve, which should be selected as close to peak efficiency as possible.

Accordingly, the system performance index (ζ_2) represents the ratio of air-side heat transfer rate to the air-side pressure drop of heat exchangers at the operating point. In this final analysis, the ζ_2 is modified by using the fan power (W_F) instead of air-side pressure drop at the operating point, as shown in Eq. (32). Therefore, the dimensionless system performance index (ζ_3) can be described as the performance of the heat exchanger.

Additionally, the ζ_3 can be defined as "Coefficient of performance" because it represents the ratio of desired output (Q_{ave}) to required input (W_F) of the system. Fig. 8 shows the variation in the fin pitch of an axial commercial fan curve (A to C) on the performance index (ζ_3) at the operating point. It can be clearly seen from the figure, the ζ_3 of a lower-input power fan is always higher than the ζ_3 of higher-input power fans. The result shows the same trend for the ζ_3 in different types of fan curves.

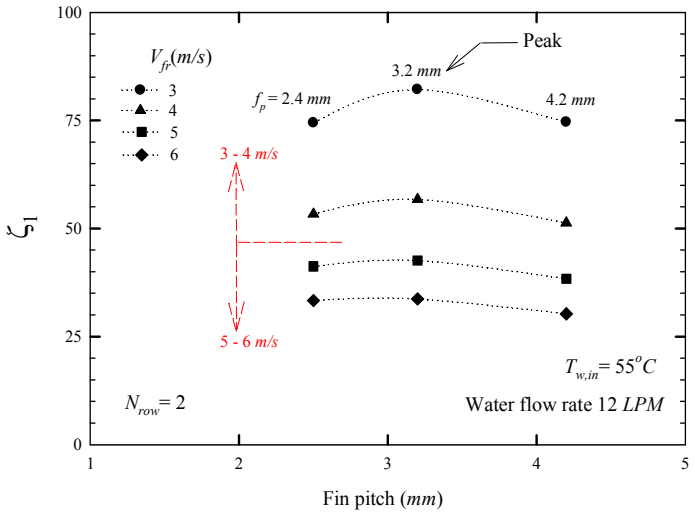

(a)

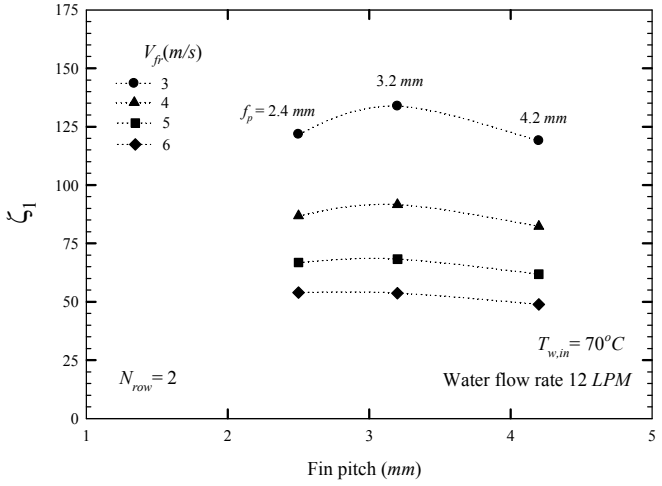

(b)

FIGURE 5 EFFECT OF FIN PITCH ON THE HEAT EXCHANGER PERFORMANCE INDEX ζ_1 HAVING DIFFERENT INLET-WATER TEMPERATURES (a) 55 °C AND (b) 70 °C.

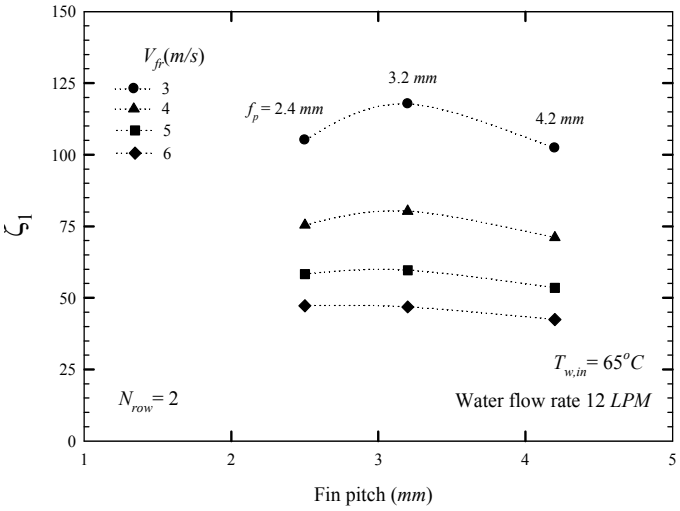

(a)

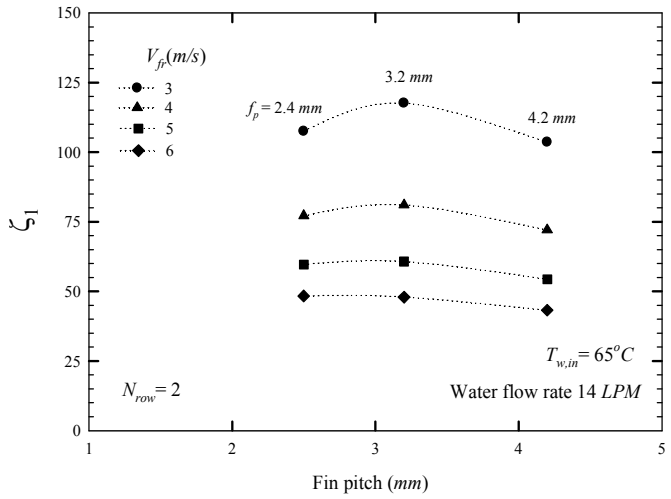

(b)

FIGURE 6 EFFECT OF FIN PITCH ON THE HEAT EXCHANGER PERFORMANCE INDEX ζ_1 HAVING DIFFERENT WATER FLOW RATES (a) 12 *LPM* AND (b) 14 *LPM*.

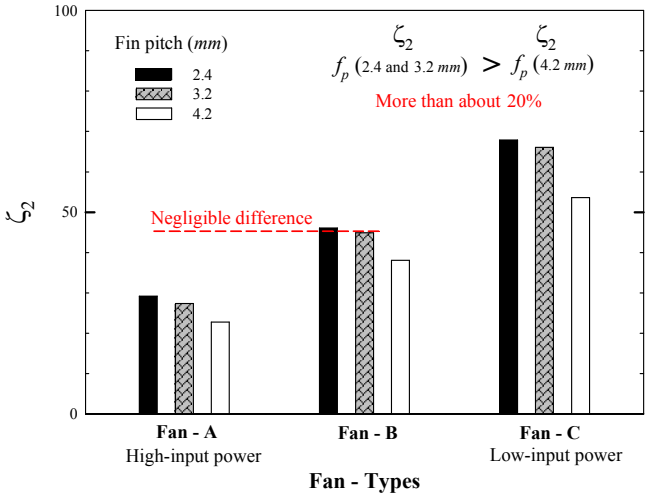

FIGURE 7 EFFECT OF FIN PITCH SUBJECTED TO FAN CURVE ON THE PERFORMANCE INDEX ζ_2 AT OPTIMUM FAN OPERATING POINT ($T_{w,in}$ = 55 ^oC AND WATER FLOW RATE OF 14 *LPM*).

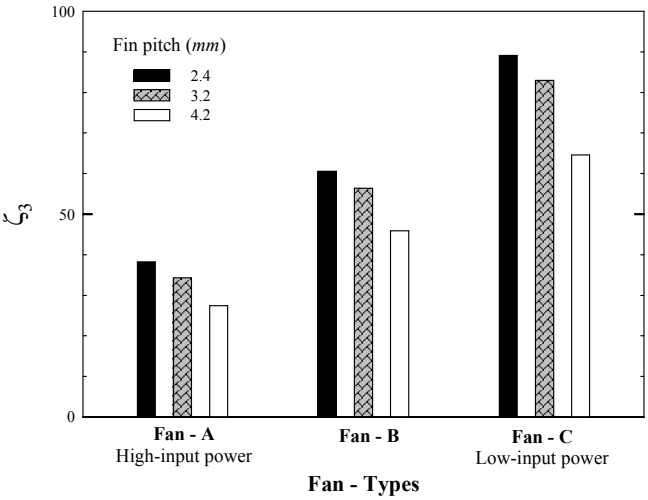

FIGURE 8 EFFECT OF FIN PITCH SUBJECTED TO FAN POWER ON THE PERFORMANCE INDEX ζ_3 AT OPTIMUM FAN OPERATING POINT ($T_{w,in}$ = 55 ^oC AND WATER FLOW RATE OF 14 *LPM*).

In addition, when the f_p decreases from 4.2 mm to 2.4 mm, the ζ_3 increases by about 25% (for f_p = 3.2 mm) and 35% (for f_p= 2.4 mm), respectively, compared with the ζ_3 of the fin pitch of 4.2 mm over the range of experimental conditions. Again, considering the performance indices (ζ_1 and ζ_2), we found that fin pitches of 2.4 and 3.2 mm seemed to have higher values in the performance indexes than that of 4.2 mm. This result indicates the optimized fin pitch for heat exchangers. However, the dimensionless system performance indices (ζ_3) for fin pitches of 2.4 and 3.2 mm seem to represent the highest and the intermediate performance of heat exchangers, respectively.

As mentioned, these results show the effect of fin pitch on three performance indices, which were analyzed based on the ratio of the desired output to the required input. The heat exchanger performance index (ζ_1), the system performance index (ζ_2), and the dimensionless system performance index (ζ_3) were used to discover the optimum fin pitch in this study. Therefore, as shown in Table 5, we noted the performance indices (ζ_1, ζ_2, and ζ_3) and compared them for fin pitches of 2.4, 3.2, and 4.2 mm to investigate the optimum fin pitch of L-footed spiral fin-and-tube heat exchangers. The fin pitch of 4.2 mm was clearly inferior to the other fin pitches. The three performance indices were analyzed with the intersection-of-sets method for presenting the optimum fin pitch. It is an effective tool for comparing the three performance indices based on different fin pitches. In the same manner, a fin pitch of 4.2 mm is not suitable for the design of heat exchangers. However, fin pitches of 2.4 and 3.2 mm seem to be the optimum fin pitches.

Using the VG-1 criteria, a comparison is done between the total heat transfer area of the L-footed spiral fin and the reference fin (i.e., the plain fin) by keeping the heat transfer rate, temperature difference of the fluids, and fan power constant. Considering those constant parameters in the case of VG-1, the following ratio can be expressed

$$\frac{A_{L-footed}}{A_{plain}} = \left(\frac{f_{L-footed}}{f_{plain}}\right)^{1/2}\left(\frac{j_{plain}}{j_{L-footed}}\right)^{3/2}, \qquad (33)$$

TABLE 5 CHARACTERISTICS OF FIN PITCH AND NUMBER OF TUBE ROW ON PERFORMANCES INDEXES

Geometric parameter Fin pitch (*mm*)	Heat exchanger performance index (ζ_1)	System performance index (ζ_2)	Dimensionless system performance index (ζ_3)
2.4*	Intermediate*	High*	High*
3.2*	High*	High*	Intermediate*
4.2	Low	Low	Low

Note: *Optimum condition.

TABLE 6 AIR-SIDE PERFORMANCE CORRELATIONS OF THE PLAIN, CRIMPED AND L-FOOTED SPIRAL FINNED TUBE HEAT EXCHANGERS

Round tube				
Authors	**Fin types**	**Surface condition**	**Correlations**	**Range of parameters /Comment**
Wang and Chang [22]	Plain fin	Dry surface	j - Colburn factor correlation $\frac{j_N}{j_4} = 0.991\left[2.24Re_{do}^{-0.092}\left(\frac{N_{row}}{4}\right)^{-0.031}\right]^{0.607(4-N_{row})}$ $j_4 = 0.14Re_{do}^{-0.328}\left(\frac{P_T}{P_L}\right)^{-0.502}\left(\frac{f_p}{d_o}\right)^{0.0312}$	$Re_{do} = 300-8000$ $d_o = 7-19.51$ mm $f_p = 1.07-8.51$ mm $N_{row} = 1-8$ $P_T = 20.35-50.73$ mm $P_L = 12.7-44.09$ mm
Wang et al. [23]	Plain fin	Dry surface	f - friction factor correlation $f = 1.039Re_{do}^{-0.418}\left(\frac{f_t}{d_o}\right)^{-0.104}N_{row}^{-0.0935}\left(\frac{f_p}{d_o}\right)^{-0.197}$	$Re_{do} = 800-7500$ $d_o = 10.51$ mm $f_p = 1.77-3.21$ mm $N_{row} = 2-6$ $P_T = 25.4$ mm $P_L = 22$ mm
Pongsoi et al. [21]	Crimped spiral fin	Dry surface	j - Colburn factor and f-friction factor correlations $j = 0.4132Re_{do}^{-0.4287}$ $f = 0.3775Re_{do}^{-0.1485}\left(\frac{f_p}{d_o}\right)^{0.4321}$	$Re_{do} = 3000-13000$ $d_o = 16.35$ mm $f_p = 2.4-6.3$ mm $N_{row} = 2-5$ $P_T = 39$ mm $P_L = 35$ mm
Pongsoi et al. [6]	L-footed spiral fin	Dry surface	j - Colburn factor and f-friction factor correlations $j = 0.2150Re_{do}^{-0.4059}$ $f = 0.4852Re_{do}^{-0.2156}\left(\frac{f_p}{d_o}\right)^{0.4771}$	$Re_{do} = 4000-15000$ $d_o = 16.35$ mm $f_p = 2.4-4.2$ mm $N_{row} = 2$ $P_T = 39$ mm $P_L = 35$ mm

Notes: Correlations are based on staggered layout.

where $A_{L\text{-}footed}$ and A_{plain} are areas of the L-footed spiral fin and plain fin geometries, respectively. The area ratio is related to the ratios for the Colburn factor and the friction factor; it also measures the possible reduction of the heat transfer area.

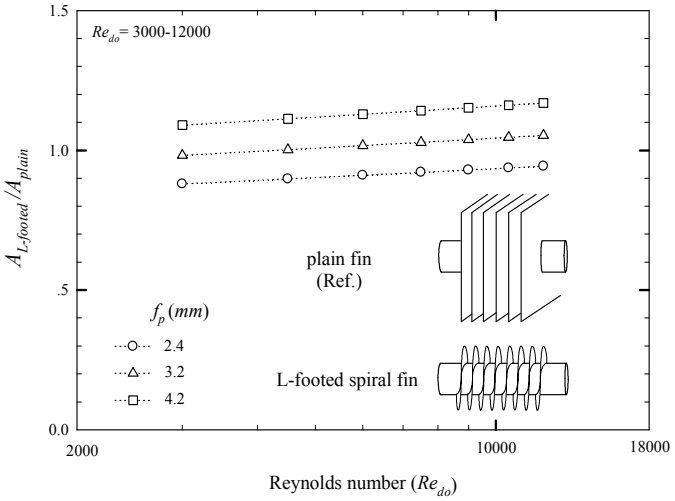

FIGURE 9 RATIO OF AIR-SIDE HEAT TRANSFER AREA OF L-FOOTED SPIRAL FIN WITH RELATION TO THE PLAIN SPIRAL FIN.

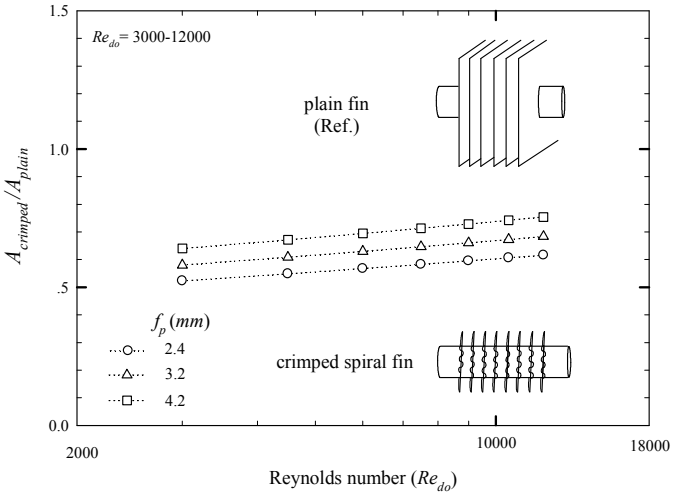

FIGURE 10 RATIO OF AIR-SIDE HEAT TRANSFER AREA OF CRIMPED SPIRAL FIN WITH RELATION TO THE PLAIN SPIRAL FIN.

In addition, the *j*-Colburn and *f*-friction factor correlations for the L-footed spiral fin, crimped spiral fin, and plain fin-and-tube heat exchangers, which were proposed by Pongsoi et al. [6], Pongsoi et al. [21], Wang and Chang [22], and Wang et al. [23], respectively, are shown in Table 6. These correlations were selected for comparison with the tested results. In Fig. 9, the VG-1 criterion covers the research findings on the comprehensive comparison between the L-footed spiral fin and plain fin for three different fin pitches varying from 2.4 mm to 4.2 mm. The effects of the fin pitches and Reynolds numbers on the variations of the area ratios, as compared with the plain fin (reference fin), the L-footed-to-plain fins heat transfer area ratio increased as the Reynolds number increased. Moreover, the L-footed-to-plain fins heat transfer area ratio increased when f_p increased from 2.4 mm to 4.2 mm. At the same Reynolds number, the L-footed fins clearly require about 6–13% less heat transfer area than the plain fin for f_p = 2.4 mm, the same heat transfer area as the plain fin for f_p = 3.2 mm, and 9–16% more heat transfer area than the plain fin for f_p = 4.2 mm to yield the same air-side heat transfer performance. Thus, smaller fin pitch presents better performance and requires less area.

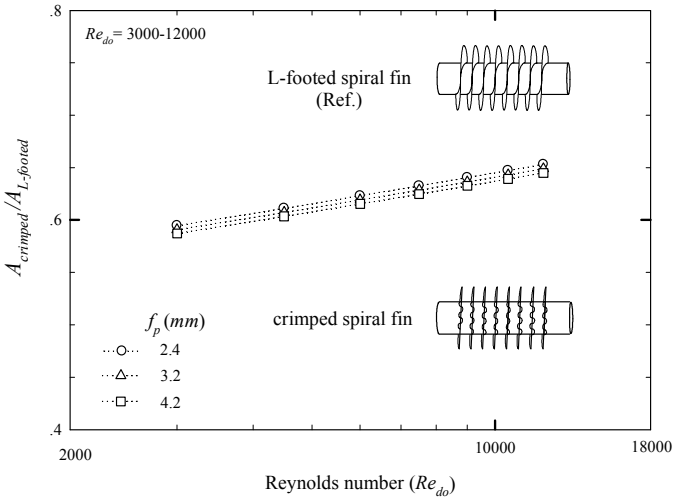

FIGURE 11 RATIO OF AIR-SIDE HEAT TRANSFER AREA OF CRIMPED SPIRAL FIN WITH RELATION TO THE L-FOOTED SPIRAL FIN.

In a comparison between the crimped spiral fin and plain fin configurations, the researchers found that the crimped spiral fin needs less heat transfer area than that of the plain fin: about 39–48% for f_p = 2.4 mm, 32–42% for f_p=3.2 mm, and 25–36% for f_p = 4.2 mm, as shown in Fig. 10. As demonstrated in Fig. 11, the test results also indicate that the effect of fin pitch on the crimped-to-L-footed spiral fins' heat transfer area ratio is very small. As expected, the crimped fin requires about 50–70% less heat transfer area than that of the L-footed spiral fin for all fin pitches (f_p = 2.4, 3.2, and 4.2 mm), as analyzed according to the VG-1 criteria and reported by Webb [24]. This may be because the crimped spiral fin mixes the turbulent flow across the spaces between fins more effectively than the plain fin and L-footed spiral fin. However, due to the specific configuration of the base of the crimped spiral finned tube, it appears that the crimped spiral fins drop pressure more than plain and L-footed spiral fins do at the same Reynolds number.

CONCLUSION

In this study, optimized fin pitches for L-footed spiral fin-and-tube heat exchangers were investigated experimentally at 2.4, 3.2, and 4.2 mm (i.e., 10, 8, and 6 fpi), respectively. The heat exchanger design usually involves three performance indices (ζ_1, ζ_2, and ζ_3). The findings are as follows:

- Variations in fin pitch had a significant effect on the three performance indices.
- For the heat exchanger performance index (ζ_1), we found that ζ_1 reaches its optimum level at a fin pitch of 3.2 mm.

However, the effect of fin pitch on ζ_1 can be neglected in a frontal velocity range of 5–6 m/s.

- The system performance index ζ_2 at fin pitches of 2.4 and 3.2 *mm* is higher than that at 4.2 *mm* by about 20%.
- The dimensionless system performance index (ζ_3) decreases as fin pitch increases.
- The optimum fin pitches were 2.4 and 3.2 mm. These values are important to the design of heat exchangers and related applications in industry.

NOMENCLATURE

A	area, m^2
A_{min}	minimum free flow area, m^2
A_o	total surface area, m^2
A_p	cross-sectional or profile area of fin, m^2
c_p	specific heat at constant pressure, $J/(kg.K)$
C	heat capacity rate, W/K
C^*	capacity rate ratio, dimensionless
C_c	cold-fuid capacity rate, W/K
C_h	hot-fluid capacity rate, W/K
COP	coefficient of performance, dimensionless
Cu	copper
d_f	outside diameter of fin, m
d_i	tube inside diameter, m
d_o	tube outside diameter, m
f	Fanning friction factor, dimensionless
f_p	fin pitch, m
f_t	fin thickness, m
fpi	fin per inch
G_c	mass flux of the air based on minimum free flow area, $kg/m^2.s$
H	height, m
h	heat transfer coefficient, $W/(m^2.K)$
I_0	modified Bessel function solution of the first kind, order 0
I_1	modified Bessel function solution of the first kind, order 1
k	thermal conductivity, $W/(m.K)$
K_0	modified Bessel function solution of the second kind, order 0
K_1	modified Bessel function solution of the second kind, order 1
L	length, m
m	mass flow rate, kg/s
n_t	number of tubes in row
N_{row}	number of tube rows
NTU	number of transfer units, dimensionless
P_L	longitudinal tube pitch, m
P_t	transverse tube pitch, m
Pr	Prandtl number, dimensionless
Q	heat transfer rate, W
r_o	radius of tip fin, m
r_i	radius of base fin, m
R	radius function in terms of the radius ratio, dimensionless
Re_{di}	Reynolds number based on tube inside diameter (d_i) , dimensionless
Re_{dc}	Reynolds number based on fin collar outside diameter (d_c) , dimensionless
T	temperature, ^oC
T_w	water temperature, ^oC
U	overall heat transfer coefficient, $W/(m^2.K)$
V_i	velocity based on tube inside diameter (d_i), m/s
V_{fr}	air frontal velocity, m/s
W	power, W

Greek symbols

ε	heat exchanger effectiveness, dimensionless
η	fin efficiency, dimensionless
η_o	overall surface effectiveness, dimensionless
ρ	density, kg/m^3
σ	contraction ratio of cross-sectional area, dimensionless
μ	dynamic viscosity of air, $Pa.s$
ϕ	combination of terms, dimensionless
ψ	radius ratio, dimensionless
ΔP	pressure drop, Pa
ζ_1	heat exchanger performance index, W/Pa
ζ_2	system performance index, W/Pa
ζ_3	dimensionless system performance index dimensionless

Subscripts

1	air-side inlet
2	air-side outlet
a	air
ave	average
b	unfinned base surface
c	multipass counter cross flow or cold fluid
crimped	crimped spiral fin
f	fin
F	fan
fr	frontal ($L \times H$)
h	hot fluid
i	tube-side
in	inlet
L-footed	L-footed spiral fin
m	mean value
max	maximum
min	minimum
o	air-side
p	multipass parallel cross flow
plain	plain fin
pc	multipass parallel-and-counter cross flow
t	tube
w	water

ACKNOWLEDGMENTS

The authors are indebted to the Thailand Research Fund, the National Science and Technology Development Agency and the National Research University Project for the support.

REFERENCES

[1] S.B. Genic, B.M. Jacimovic, B.R. Latinovic, Research on air pressure drop in helically-finned tube heat exchangers, Applied Thermal Engineering 26 (5-6) (2006) 478-485.
[2] H. Hamakawa, K. Nakashima, T. Kudo, E. Nishida, T. Fukano, Vortex Shedding from a Circular Cylinder with Spiral Fin, Journal of Fluid Science and Technology 3 (6) (2008) 787-795.
[3] M. Lee, T. Kang, Y. Kim, Air-side heat transfer characteristics of spiral-type circular fin-and tube heat exchangers, International Journal of Refrigeration 33 (2) (2010) 313-320.
[4] M. Lee, T. Kang, Y. Joo, Y. Kim, Heat transfer characteristics of spirally-coiled circular fin-tube heat exchangers operating under frosting conditions, International Journal of Refrigeration 34 (1) (2011) 328-336.
[5] P. Pongsoi, S. Pikulkajorn, S. Wongwises, Experimental study on the air-side performance of a Multipass parallel and counter cross-flow L-footed spiral fin-and-tube heat exchanger, Heat Transfer Engineering 33 (15) (2012) 1251-1263.
[6] P. Pongsoi, P. Promoppatum, S. Pikulkajorn, S. Wongwises, Effect of fin pitches on the air-side performance of L-footed spiral fin-and-tube heat exchangers, Int. Journal of Heat and Mass Transfer 59 (2013) 75-82.
[7] C.W. Lu, J.M. Huang, W.C. Nien, C.C. Wang, A numerical investigation of the geometric effects on the performance of plate finned-tube heat exchanger, Energy Conversion and Management 52 (3) (2011) 1638-1643.
[8] R. Romero-Mendez, M. Sen, K.T. Yang, R. McClain, Effect of fin spacing on convection in a plate fin and tube heat exchanger, International Journal of Heat and Mass Transfer 43 (1)(2000) 39-51.
[9] T. Sencic, A. TRP, K. Lenic, Parametric study of operating and geometry characteristics effect on heat transfer in annular finned tube heat exchanger, Engineering Review 29 (1) (2009) 25-36.
[10] M. Lee, T. Kang, Y. Kim, Air-side heat transfer characteristics of spiral-type circular fin- and-tube heat exchangers, International Journal of Refrigeration 33 (2) (2010) 313-320.
[11] H. Hamakawa, K. Nakashima, T. Kudo, E. Nishida, T. Fukano, Vortex shedding from a circular cylinder with spiral fin, Journal of Fluid Science and Technology 3 (6) (2008) 787-795.
[12] P. Pongsoi, S. Pikulkajorn, S. Wongwises, Effect of fin pitches on the optimum heat transfer performance of crimped spiral fin-and-tube heat exchangers, Int. Journal of Heat and Mass Transfer 55 (23-24) (2012) 6555-6566.
[13] G. Xie, Q. Wang, B. Sunden, Parametric study and multiple correlations on air-side heat transfer and friction characteristics of fin-and-tube heat exchangers with large number of large-diameter tube rows, Applied Thermal Engineering 29 (1) (2009) 1-16.
[14] Y.C. Liu, S. Wongwises, W.J. Chang, C.C. Wang, Airside performance of fin-and-tube heat exchangers in dehumidifying conditions - Data with larger diameter, International Journal of Heat and Mass Transfer 53 (7-8) (2010) 1603-1608.
[15] C.C. Wang, J.S. Liaw, Air-side performance of herringbone wavy fin-and-tube heat exchangers under dehumidifying condition – Data with larger diameter tube, International Journal of Heat and Mass Transfer 55 (11-12) (2012) 3054-3060.
[16] C.C. Wang, J.S. Liaw, B.C. Yang, Airside performance of herringbone wavy fin-and-tube heat exchangers – data with larger diameter tube, International Journal of Heat and Mass Transfer 54 (5-6) (2011) 1024-1029.
[17] V. Gnielinski, New eguation for heat and mass transfer in turbulent pipe and channel flow, Int. Chem. Eng. 16 (1976) 359-368.
[18] K.A. Gardner, Efficient of Extended Surface, ASME Trans 67 (1945) 621.
[19] W.M. Kays, A. London, Compact heat exchangers, 3rd Ed., Mcgraw-Hill, New York (1984).
[20] ANSI/ASHRAE Standard 33-2000, Method of Testing Forced Circulation Air Cooling and Air Heating Coils (2000).
[21] P. Pongsoi, S. Pikulkajorn, C.C. Wang, S. Wongwises, Effect of number of tube rows on the air side performance of crimped spiral fin-and-tube heat exchangers with a multipass parallel and counter cross-flow configuration, Int. Journal of Heat and Mass Transfer 55 (4) (2012) 1403-1411.
[22] C.C. Wang, C.T. Chang, Heat and mass transfer for plate fin-and-tube heat exchangers with and without hydrophilic coating, Int. J. Heat Mass Transfer 41 (1998) 3109-3120.
[23] C.C. Wang, Y.J. Chang, Y.C. Hsieh, Y.T. Lin, Sensible heat and friction characteristics of plate fin- and-tube heat exchangers having plane fins, Int. Journal of Refrigeration 19(4) (1996) 223-230.
[24] R.L. Webb, Principles of Enhanced Heat Transfer, Wiley, New York (1994).